NIH Public Access
Author Manuscript
Mol Cancer Ther. Author manuscript; available in PMC 2012 May 1.

Published in final edited form as:
Mol Cancer Ther. 2011 May ; 10(5): 806–816. doi:10.1158/1535-7163.MCT-10-1050.

Dependence on the MUC1-C Oncoprotein in Non-Small Cell Lung Cancer Cells

Deepak Raina[3], **Michio Kosugi**[1], **Rehan Ahmad**[1], **Govind Panchamoorthy**[3], **Hasan Rajabi**[1], **Maroof Alam**[1], **Takeshi Shimamura**[1], **Geoffrey I. Shapiro**[1], **Jeffrey Supko**[2], **Surender Kharbanda**[3], and **Donald Kufe**[1]

[1]Dana-Farber Cancer Institute, Harvard Medical School, Boston, MA 02115

[2]Massachusetts General Hospital, Harvard Medical School, Boston, MA 02115

[3]Genus Oncology, Boston, MA 02118

Abstract

Non-small cell lung cancer (NSCLC) cells are often associated with constitutive activation of the phosphatidylinositol 3-kinase (PI3K)->Akt->mTOR pathway. The mucin 1 (MUC1) heterodimeric glycoprotein is aberrantly overexpressed in NSCLC and induces gene signatures that are associated with poor survival of NSCLC patients. The present results demonstrate that the MUC1 C-terminal subunit (MUC1-C) cytoplasmic domain associates with PI3K p85 in NSCLC cells. We show that inhibition of MUC1-C with cell-penetrating peptides blocks this interaction with PI3K p85 and suppresses constitutive phosphorylation of Akt and its downstream effector, mTOR. In concert with these results, treatment of NSCLC cells with the MUC1-C peptide inhibitor, GO-203, was associated with downregulation of PI3K->Akt signaling and inhibition of growth. GO-203 treatment was also associated with increases in reactive oxygen species (ROS) and induction of necrosis by a ROS-dependent mechanism. Moreover, GO-203 treatment of H1975 (EGFR L858R/T790M) and A549 (K-Ras G12S) xenografts growing in nude mice resulted in tumor regressions. These findings indicate that NSCLC cells are dependent on MUC1-C for activation of the PI3K->Akt pathway and for survival.

Keywords

MUC1; NSCLC; PI3K; EGFR; K-Ras; ROS

Introduction

Non-small cell lung cancers (NSCLC) are associated with constitutive activation of the phosphatidylinositol 3-kinase (PI3K)-Akt-mTOR pathway (1-3). The PI3K p85 regulatory subunit contains Src homology 2 (SH2) domains that interact with pYXXM sequences on activated receptor tyrosine kinases (RTKs), such as the epidermal growth factor receptor (EGFR) (4). In turn, PI3K p85-mediated inhibition of the PI3K p110 catalytic subunit is relieved and p110 phosphorylates Akt (4). PI3K p110 also binds directly to Ras, linking activation of PI3K signaling to the constitutive activation of Ras mutants (5). Effective

Requests for reprints: Donald Kufe, Dana-Farber Cancer Institute, 44 Binney Street, Dana 830, Boston, MA 02115, Phone: 617-632-3141; Fax: 617-632-2934. Donald_Kufe@dfci.harvard.edu.

Disclosure of Potential Conflicts of Interest: D. Raina, G. Panchamoorthy and S. Kharbanda: employees of Genus Oncology. D. Kufe: equity holder and consultant, Genus Oncology. J. Supko: received research support from Genus Oncology. Genus Oncology provided the peptides used in these experiments and performed the animal studies at a contract organization.

NIH-PA Author Manuscript
NIH-PA Author Manuscript
NIH-PA Author Manuscript

NIH-PA Author Manuscript

NIH-PA Author Manuscript

NIH-PA Author Manuscript

treatment of NSCLC cells with EGFR inhibitors is associated with suppression of PI3K activity and resistance to these inhibitors occurs with reactivation of the PI3K-Akt signaling pathway (4). The mTOR complex 1 (mTORC1) is a downstream effector of Akt, as well as other inputs, that regulates cell growth and is often dysregulated in human cancers (6). In this regard, agents that block the PI3K->Akt->mTOR pathway are under clinical development for the treatment of NSCLC (4). Amplification or mutation of EGFR in NSCLC has been targeted with small molecule tyrosine kinase inhibitors (erlotinib, gefitinib). The most common *EGFR* mutations consisting of L858R and exon 19 deletions confer sensitivity to erlotinib and gefitinib with increases in the frequency and duration of clinical responses (7). However, these patients ultimately develop resistance to treatment, at least in part, due to acquisition of the T790M mutation (8). Second generation irreversible EGFR inhibitors have in turn been developed for targeting the EGFR T790M mutant kinase (8, 9). About 20-30% of NSCLC express K-Ras with mutations in codons 12 or 13 (10, 11). Consistent with K-Ras functioning downstream to EGFR, NSCLC patients with K-Ras mutant tumors are unresponsive to EGFR inhibitors (12). Moreover, adjuvant chemotherapy is ineffective against NSCLCs harboring K-Ras mutations, thus limiting treatment options for these patients. The PI3K->Akt pathway is constitutively activated in NSCLC with EGFR and K-Ras mutations (4). In addition, NSCLC cells with the *EML4-ALK* fusion gene are associated with activation of PI3K->Akt signaling (13, 14), thus emphasizing the importance of this pathway as a focus of targeted therapy.

Mucin 1 (MUC1) is translated as a single polypeptide that undergoes autocleavage into N-terminal (MUC1-N) and C-terminal (MUC1-C) subunits (15). MUC1-N contains the highly glycosylated tandem repeats that are characteristic of the mucin family. By contrast, MUC1-C is a transmembrane protein that functions as a cell surface receptor (15). The MUC1-C extracellular domain interacts with the ligand galectin-3 and thereby forms complexes with EGFR (16). The available evidence indicates that MUC1-C promotes EGFR-mediated signaling (17-19). In this context, the MUC1-C cytoplasmic domain functions as a substrate for EGFR and c-Src phosphorylation (17, 20). In turn, the MUC1-C pYEKV motif serves as a binding site for the c-Src SH2 domain (20). The MUC1-C cytoplasmic domain also contains a YTNP site that, when tyrosine phosphorylated, interacts directly with the SH2 domain of the Grb2 adapter protein (21, 22). The MUC1-C/Grb2 complex associates with the Ras activator son-of-sevenless (SOS), linking MUC1-C to the Ras pathway (21). Importantly, MUC1-C activates the PI3K->Akt pathway (23) and the MUC1-C cytoplasmic domain has a YHPM site that following phosphorylation functions as a binding site for the PI3K SH2 domain (24). Overexpression of MUC1 as found in human carcinomas is associated with accumulation of MUC1-C in the cytoplasm and targeting of MUC1-C to the nucleus (15). The overexpression of MUC1-C has also been directly associated with activation of β-catenin (25), IKK->NF-κB RelA (26, 27) and STAT1/3 (28, 29) signaling. In concert with these functions, an inhibitor of MUC1-C oligomerization blocks MUC1-C-mediated activation of the NF-κB and STAT pathways (27-29). In addition, treatment of human breast and prostate tumor xenografts in nude mice with the MUC1-C inhibitors, GO-201 and GO-202, is associated with complete and prolonged regressions (30, 31). Recent work has shown that MUC1-C induces gene signatures that are highly predictive of overall and disease-free survival of NSCLC patients (32, 33). Importantly, silencing of MUC1 expression in NSCLC cells is associated with downregulation of STAT3 activation and loss of survival (34).

The present studies demonstrate that MUC1-C associates with PI3K in NSCLC cells through direct binding of the MUC1-C cytoplasmic domain and the PI3K p85 SH2 domain. The results show that inhibition of MUC1-C function blocks activation of the PI3K->p-Akt->p-mTOR pathway. The results also demonstrate that the MUC1 inhibitor, GO-203, increases ROS and induces necrotic death of NSCLC cells in vitro. Moreover, we

NIH-PA Author Manuscript

NIH-PA Author Manuscript

NIH-PA Author Manuscript

demonstrate that GO-203 is effective in inducing regressions of NSCLC tumor xenografts in mice.

Materials and Methods

Cell culture

Human H1975 (35), H1650 (ATCC) (36), HCC827 (35), A549, H2228 (13), H460 (37), H1299 (38) and NCI-H292 (39) NSCLC cells were all obtained from the ATCC and passaged for less than 6 months and then replaced with early passage frozen stocks. No further authentication was performed. The cells were grown in RPMI 1640 medium supplemented with 10% heat-inactivated fetal bovine serum (HI-FBS), 100 units/ml penicillin, 100 μg/ml streptomycin and 2 mM L-glutamine. Normal lung epithelial cells (NLEC; Lonza) were cultured in epithelial cell growth medium. Cells were treated with GO-201, GO-202, GO-203, CP-1 and CP-2 peptides (AnaSpec, Inc.; all dissolved in PBS), N-acetylcysteine (NAC; Sigma) and Tiron (Sigma). Viability was determined by trypan blue exclusion. Cells were transiently transfected with small interfering RNA (siRNA) pools (Dharmacon) in the presence of Lipofectamine 2000 (Invitrogen).

Immunoprecipitation and immunoblot analysis

Cell lysates were prepared as described (30). Soluble proteins were immunoprecipitated with anti-MUC1-C (Ab5; Neomarkers), anti-EGFR (Abcam) or a control IgG. The precipitates and lysates not subjected to immunoprecipitation were immunoblotted with anti-MUC1-C, anti-β-actin (Sigma-Aldrich), anti-p-EGFR (Cell Signaling Technology), anti-EGFR, anti-p-Akt, anti-Akt, anti-p-mTOR, anti-mTOR (Cell Signaling Technology), anti-PI3K p85 (Millipore) and anti-P-Tyr (4G10; Millipore). Reactivity was detected with horseradish peroxidase-conjugated secondary antibodies and chemiluminescence.

Quantitative RT-PCR

Total RNA was isolated from cells using the RNeasy Mini Kit (Qiagen). For real time qRT-PCR, cDNA synthesis was performed with 1 μg of total RNA using the Superscript-III First-Strand Synthesis SuperMix (Invitrogen). The SYBR green qPCR assay kit (Applied Biosystems) was used with 1 μl of cDNA for amplification with the ABI Prism 7000 Sequence Detector (Applied Biosystems). Primers used for qRT-PCR are listed in the Supplemental Table. Relative Enrichment was calculated as described (28) and the results are expressed as the mean±SD of triplicate values for each sample.

In vitro binding assays

GST and GST-PI3K p85 SH2 (Pierce Biotechnology) were bound to glutathione beads and incubated with cell lysates as described (26). Alternatively, purified His-MUC1-CD was incubated with recombinant c-Met (Upstate Cell Signaling Solutions) in kinase buffer containing 15 μM ATP for 15 min at room temperature. Samples were washed and then incubated with GST or GST-PI3K p85 SH2. Adsorbates were analyzed by immunoblotting.

Cell transfections

HEK293 cells were transfected with pIRES-puro2-MUC1 or pIRES-puro2-MUC1(Y20F) in the presence of Lipofectamine as described (40). The cells were harvested at 48 h after transfection for coimmunoprecipitation studies.

Analysis of cell cycle distribution and cell membrane integrity

Cells were fixed with 80% ethanol and incubated in PBS containing RNase and propidium iodide (PI) as described (30). Cell cycle distribution and sub-G1 DNA content were

NIH-PA Author Manuscript

NIH-PA Author Manuscript

NIH-PA Author Manuscript

determined by flow cytometry. For assessment of cell membrane integrity, cells were incubated with 1 μg/ml PI/PBS for 5 min at room temperature and then monitored by flow cytometry as described (30).

Measurement of ROS levels

Cells were incubated with 10 μM c-H_2DCFDA (Molecular Probes) for 20 min at 37°C. Fluorescence of oxidized c-H_2DCF was measured as described (31).

NSCLC tumor xenograft models

Four to six week old BALB/c nu/nu male/female mice were injected subcutaneously with 1 × 10^7 H1975 or A549 cells in the flank. When tumors were detectable, the mice were pair matched into control and treatment groups of 10 mice each. Mice were excluded if the tumors were not within 15% of the mean volume. PBS (control vehicle), 30 mg/kg body weight GO-203 or 30 mg/kg body weight CP-2 (peptides dissolved in PBS) were administered daily by intraperitoneal injection for 21 d. Tumor volume (V) was calculated using the formula $V=L^2 \times W/2$, where L and W are the larger and smaller diameters, respectively. Tumors and sites of tumor implantation were evaluated by staining with H&E.

Statistical analysis

Analysis of data was performed using the two-tailed, unpaired Student's *t* test. *P* values greater that $p<0.05$ were considered significant.

Results

Effects of inhibiting MUC1-C with GO-201 on growth and survival of NSCLC cells

Previous work has shown that MUC1-C is expressed in NSCLC cell lines (34). In concert with those findings, immunoblot analysis of H1975 (EGFR L858R/T790M), H1650 (EGFR delE746-A750) and HCC827 (EGFR delE746-A750) NSCLC cells confirmed expression of the MUC1-C subunit (Fig. 1A). To assess sensitivity to inhibition of MUC1 function, H1975 cells were treated with the MUC1-C peptide inhibitors, GO-201 ($[R]_9$-CQCRRKNYGQLDIFP) and GO-202 ($[R]_9$-CQCRRKN) that contain amino acids derived from the MUC1-C cytoplasmic domain (Fig. 1B). The 9 Arg residues linked at the N-terminus have been shown to confer cell penetration (30). As a control, the cells were treated with CP-1, an inactive form in which the CQC motif has been altered to AQA ($[R]_9$-AQARRKNYGQLDIFP) (Fig. 1B) (30). Treatment of H1975 cells with 5 μM GO-201 or GO-202 was associated with an initial inhibition of growth and then a decrease in cell number (Fig. 1B). By contrast, CP-1 had little if any effect (Fig. 1B). H1650 and HCC827 cells also responded to GO-201 and not CP-1 with suppression of growth (Fig. 1C). Similar results were obtained with HCC827 cells (Fig. 1D). These findings indicated that MUC1-C is a potential target for certain NSCLC cells with activating EGFR mutations.

GO-203 inhibits growth and survival of NSCLC cells

Human A549 NSCLC cells harbor a K-Ras G12S mutation and express MUC1-C at elevated levels compared to that in normal lung epithelial cells (NLEC) (Fig. 2A). Growth of A549 cells was substantially inhibited by GO-201 and a shorter version, GO-202 (Fig. 2B). Conversion of GO-202 to the D-amino acid configuration, designated GO-203, was then tested to determine whether such modification affects activity. In this regard, like GO-201 (30), GO-203 blocked oligomerization of the MUC1-C cytoplasmic domain (Supplemental Fig. S1). Moreover, GO-203 was effective in inhibiting A549 cell growth (Fig. 2C, left). Using a control peptide, designated CP-2, alteration of the CQC motif to AQA abrogated the growth inhibitory effects (Fig. 2C, left). In contrast to the effects on A549 cells, GO-203 had

NIH-PA Author Manuscript

NIH-PA Author Manuscript

NIH-PA Author Manuscript

no significant effect on NLEC growth (Fig. 2C, right). Human H2228 NSCLC cells have the *EML4-ALK* translocation and express MUC1-C at somewhat higher levels than that in H1650 cells (Fig. 2D, left). As found for A549 cells, H2228 cells were also sensitive to GO-202 and GO-203 (Fig. 2D, right), further indicating that the D-amino acid configuration is as active as the L-form. Indeed, growth of H1975, H1650 and HCC827 cells was similarly inhibited by GO-203 (data not shown).

To further assess sensitivity of NSCLC cells to GO-203, we studied NCI-H292 (wild-type EGFR, wild-type K-Ras), H1299 (wild-type EGFR, wild-type K-Ras) and H460 (wild-type EGFR, K-Ras G61H) NSCLC cells. As compared to that in A549 cells, MUC1 mRNA levels were higher in NCI-H292 cells and similar in H1299 cells (Supplemental Fig. S2A). By contrast, H460 cells had a lower abundance of MUC1 mRNA (Supplemental Fig. S2A). Immunoblot analysis confirmed a relatively higher level of MUC1-C protein in NCI-H292 cells as compared to that in H1299 and H460 cells (Supplemental Fig. S2B). NCI-H292 and H1299 cells responded to GO-203 treatment with an initial slowing of growth and then a decline in cell number over days 4 to 8 (Supplemental Figs. S2C and D). Growth of H460 cells, which express relatively lower levels of MUC1-C, was also slowed; however, there was no significant decrease in cell number after day 4 (Supplemental Fig. S2E). These findings indicate that (i) sensitivity of NSCLC cells to GO-203 is independent of the EGFR or K-Ras mutational status, and (ii) a level of MUC1-C expression below a certain threshold, as observed in H460 cells, may confer less dependence on MUC1-C for survival.

MUC1 levels have been shown to be independent of EGFR expression in NSCLC (41). To assess the effects of EGFR on MUC1-C, we downregulated EGFR with siRNA pools in H1975 cells (Supplemental Fig. S3A). Silencing EGFR had no detectable effect on MUC1-C abundance (Supplemental Fig. S3A). Silencing of K-Ras in A549 cells also had no effect on MUC1-C levels (Supplemental Fig. S3B), indicating that MUC1-C expression is independent of EGFR and K-Ras signaling in these cells.

GO-203 disrupts the interaction between MUC1-C and PI3K p85

The MUC1-C cytoplasmic domain associates with PI3K p85 in transfected HEK293 cells (24). To determine whether endogenous MUC1-C associates with PI3K in NSCLC cells, coprecipitation studies were performed using using H1975 cell lysates. The results demonstrated that MUC1-C associates with PI3K p85 (Fig. 3A). Moreover, treatment of the H1975 cells with GO-203, but not CP-2, blocked the interaction between MUC1-C and PI3K p85 (Fig. 3A). Similar results were obtained in coprecipitation experiments using A549 cell lysates (Fig. 3B). The MUC1-C cytoplasmic domain contains a YHPM motif that, when phosphorylated, functions as a binding motif for the PI3K p85 SH2 domains (Fig. 3C). To determine whether GO-203 blocks the direct interaction, we first incubated the MUC1-C cytoplasmic domain with the PI3K p85 SH2 domain. As expected, there was no detectable binding (Fig. 3C, left). However, in concert with previous studies demonstrating that the YHPM site is phosphorylated by c-Met (15), recombinant c-Met-mediated phosphorylation of the YHPM site was associated with binding to the PI3K p85 SH2 domain (Fig. 3C, left). In addition, the interaction between the phosphorylated MUC1-C cytoplasmic domain and PI3K p85 SH2 was attenuated by including increasing amounts of GO-203 to the reactions (Fig. 3C, right). As further evidence for involvement of the pYHPM motif, mutation of the MUC1-C cytoplasmic domain at Y-20 to F (Y20F) blocked the interaction with PI3K p85 SH2 (Fig. 3D, left). Transfection of MUC1-null 293 cells with a vector expressing MUC1 or MUC1(Y20F) also showed that coprecipitation of MUC1-C with PI3K p85 is abrogated by the Y20F mutation (Fig. 3D, right). These findings indicated that MUC1-C associates with PI3K through direct binding to the pYHPM motif in the MUC1-C cytoplasmic domain and that GO-203 blocks the interaction.

NIH-PA Author Manuscript

NIH-PA Author Manuscript

NIH-PA Author Manuscript

Treatment of H1975 or A549 cells with GO-203 had no effect on the interaction between EGFR and PI3K p85, indicating that the inhibitory effects of GO-203 on the PI3K->Akt->mTOR pathway are not attributable to disruption of the interaction between PI3K p85 and EGFR (Supplemental Figs. S4A and B). Moreover, GO-203 treatment of H1975 cells was associated with a modest decrease in phosphorylation of MUC1-C on tyrosine (Supplemental Fig. S4C) and no apparent effect on MUC1-C tyrosine phosphorylation in A549 cells (Supplemental Fig. S4D).

Inhibition of MUC1-C downregulates the PI3K->Akt pathway

Based on the above observations, we asked if disruption of the interaction between MUC1-C and PI3K p85 with GO-203 affects phosphorylation of Akt. Significantly, treatment of H1975 cells with GO-203, and not CP-2, was associated with inhibition of Akt phosphorylation, consistent with downregulation of PI3K signaling (Fig. 4A). Treatment with GO-203 was also associated with inhibition of the PI3K-related mTOR pathway (Fig. 4A). Moreover, GO-203 was effective in downregulating p-Akt and p-mTOR in H1650 and HCC827 cells (Fig. 4B), indicating that inhibition of MUC1-C suppresses PI3K activity in these NSCLC cells with EGFR mutations. In A549 cells, GO-203 treatment was similarly associated with suppression of p-Akt and p-mTOR levels, providing further support for downregulation of PI3K activity (Fig. 4C, left). In addition and as found in H1975 cells, GO-203-induced downregulation of p-Akt and p-mTOR in A549 cells was detectable at 24 and 48 h (Fig. 4C, right), preceding the onset of cell death. Consistent with effects that extend beyond NSCLC cells with EGFR or K-Ras mutations, H2228 cells with the *EML4-ALK* translocation responded to GO-203, and not CP-2, with decreases in Akt and mTOR phosphorylation (Fig. 4D). These findings indicate that inhibition of MUC1-C in diverse types of NSCLC cells blocks the interaction between MUC1-C and PI3K p85 and suppresses activation of the PI3K->Akt->mTOR pathway.

GO-203 induces necrotic cell death by a ROS-mediated mechanism

Inhibition of the PI3K signaling pathway in NSCLC cells expressing mutant EGFR or K-Ras leads to growth arrest and not cell death (42-44). In this regard, the above studies demonstrated that inhibition of MUC1-C in H1975 and A549 cells is associated with an initial slowing of growth and then a subsequent decrease in cell number consistent with cell death. Indeed, treatment of H1975 and A549 cells with MUC1-C inhibitors for 6 days was associated with (i) extensive DNA degradation, (ii) no identifiable sub-G1 peak and (iii) loss of cell membrane integrity (Supplemental Figs. S5A and B; and data not shown), consistent with the induction of necrotic cell death. Other work has demonstrated that inhibition of MUC1-C increases ROS (30, 31); however, it is not known if disruption of redox balance in this setting contributes to cell death. To address this possibility, H1975 cells were treated with GO-203 and the antioxidant NAC. Analysis of ROS levels demonstrated that GO-203-induced increases in ROS are reversed by cotreatment with NAC (Fig. 5A). GO-203-induced necrosis of H1975 cells was also attenuated by NAC (Fig. 5B). To search for further evidence for involvement of ROS, H1975 cells were treated with Tiron, a superoxide scavenger. As found with NAC, Tiron blocked the GO-203-induced increases in ROS levels (Fig. 5C) and necrotic cell death (Fig. 5D). These findings and similar results in A549 cells (data not shown) indicated that GO-203 induces necrosis, at least in part, by a ROS-mediated mechanism.

GO-203 induces regressions of established NSCLC tumors

To assess the anti-tumor effects of GO-203, H1975 cells were implanted in the flanks of nude mice. Mice bearing tumors of ~125 mm^3 were treated ip with GO-203 and, as a control, CP-2 at a dose of 30 mg/kg/d for 21 days. GO-203, but not CP-2, treatment was associated with an initial inhibition of H1975 tumor growth and then a progressive decline

NIH-PA Author Manuscript

NIH-PA Author Manuscript

NIH-PA Author Manuscript

in volume (Fig. 6A). By day 28, the GO-203-treated tumors were no longer palpable (Fig. 6A). One mouse from the GO-203-treated group was sacrificed on day 32 to assess residual tumor. There was no gross evidence for remaining tumor at the implantation site or metastases to the liver, lungs and other organs. Histologic examination of the implantation site following GO-203 treatment identified a small cluster of remaining tumor cells that appeared necrotic. Notably, there was no recurrence of tumor as of day 180 when the mice were sacrificed. Treatment of established A549 tumors (~75 mm^3) with GO-203 for 21 d was similarly associated with an initial slowing of growth and then regression (Fig. 6C). Examination of the implantation site in one of the GO-203-treated mice on day 36 demonstrated necrotic debris without intact tumor cells (Fig. 6D). In addition, there was no evidence for metastatic spread. As of day 180, the other GO-203-treated mice were without recurrence, indicating that both H1975 and A549 tumors respond to GO-203 with prolonged complete regressions.

Discussion

MUC1-C cytoplasmic domain interacts with PI3K in NSCLC cells

Transformation induced by the MUC1-C subunit cytoplasmic domain is associated with activation of the PI3K->Akt pathway (23, 25). However, it was not known whether the MUC1-C subunit interacts with PI3K in NSCLC cells, which are dependent on PI3K->Akt signaling for survival. The present studies support a model in which MUC1-C activates PI3K in NSCLC cells through a direct interaction. The results show that (i) MUC1-C associates with PI3K p85 in NSCLC cells and (ii) in concert with previous work (24), the MUC1-C cytoplasmic domain pYHPM motif functions as a binding site for the PI3K p85 SH2 domain. Proteins containing the pYXXM sequence have a high affinity for the PI3K N-terminal and C-terminal SH2 domains. Specifically, ErbB3 contains 6 YXXM motifs that when phosphorylated on tyrosine function as binding sites for PI3K (4, 45). Other activated RTKs, the adaptor molecule Grb2-associated binding protein 1, and the polyoma middle T antigen also contain pYXXM sites for PI3K binding (4, 45). The present results provide evidence that the MUC1-C cytoplasmic domain plays a similar role in interacting with PI3K in NSCLC cells. The MUC1-C transmembrane receptor is positioned at the apical cell membrane of polarized epithelial cells and is sequestered from RTKs at the basolateral membranes (46). However, with loss of polarity associated with transformation, MUC1-C forms complexes with ErbB family members, FGFR3, PDGFR and c-Met, that in turn induce tyrosine phosphorylation of the MUC1-C cytoplasmic domain (15). Thus, direct binding of PI3K p85 to MUC1-C with a phosphorylated YHPM motif could confer the conformational change in p85 that activates the PI3K p110 catalytic subunit. The interaction between MUC1-C and RTKs is transient in the epithelial stress response with reversible loss of polarity (15). By contrast, in carcinoma cells with irreversible loss of polarity, the constitutive interaction between MUC1-C and RTKs could contribute to aberrant activation of the PI3K->Akt pathway that has been identified in diverse cancers.

Inhibition of MUC1-C downregulates the PI3K pathway

Dimerization of MUC1-C is dependent on a CQC motif in the cytoplasmic domain and is necessary for interactions between MUC1-C and certain effectors, such as NF-κB RelA and STAT1/3 (27-29). GO-201 is a cell-penetrating peptide that contains the CQC sequence and binds directly to the MUC1-C cytoplasmic domain, thus blocking oligomerization (30). A second-generation configuration, GO-203, was synthesized with all D-amino acids that can afford greater stability in the presence of peptidases and, like GO-201 (30), was found to block dimerization of the MUC1-C cytoplasmic domain. Our results show that (i) GO-203 is as effective as GO-201 in inhibiting NSCLC cell growth and survival, and (ii) treatment of NSCLC cells with GO-203 blocks the interaction between MUC1-C and PI3K p85. Similar

NIH-PA Author Manuscript

NIH-PA Author Manuscript

NIH-PA Author Manuscript

results were obtained with GO-203 in in vitro binding studies of MUC1-C and PI3K p85 SH2, indicating that MUC1-C oligomerization and the pYHPM motif are both needed to confer the interaction with PI3K p85. Alternatively, binding of GO-203 to the MUC1-C cytoplasmic domain could alter the conformation of the pYHPM site and thereby block binding to the PI3K p85 SH2 domain. There are a number of PI3K inhibitors that are under clinical development that directly target PI3K p110 activity (4). The evidence presented here indicates that GO-203 also blocks PI3K p110 activity; however, this effect would be indirect, that is by abrogating the interaction between the MUC1-C cytoplasmic domain and PI3K p85. Inhibition of MUC1-C was effective in suppressing p-Akt in H1975 cells and thus occurred in a setting of resistance to EGFR inhibitors. GO-203-induced downregulation of p-Akt was also found in A549 cells that harbor a K-Ras mutant, against which there are presently no effective targeted therapies. Akt functions as an activator of the mTOR complex 1 (mTORC1) and inhibitors are under development that block both PI3K and mTOR activity. In this regard, mTORC1 is also regulated by other signals; for example, the LKB1-AMPK pathway that links cell metabolism with growth control (47). Significantly, like inhibition of p-Akt, GO-203 treatment was associated with downregulation of p-mTOR in both H1975 and A549 cells. The inhibition of p-mTOR is explained, at least in part, by the effects of GO-203 on p-Akt; however, the present results do not exclude the possibility that blocking MUC1-C function may affect other signals that activate mTORC1.

GO-203 is effective in inducing death of NSCLC cells

The finding that inhibition of MUC1-C suppresses growth of NSCLC cells, without or with EGFR and K-Ras mutations, is in concert with downregulation of the PI3K->Akt pathway (1-3, 42-44). Indeed, our results indicate that the inhibitory effects of the MUC1-C peptides are dependent on MUC1-C expression and are not due to the specific gene mutation status. Nonetheless, the effects of GO-203 on PI3K signaling were not sufficient to explain the associated loss of survival in that downregulation of this pathway in NSCLC cells with EGFR or K-Ras mutations results in growth arrest and not cell death (42-44). Accordingly, the findings that MUC1 suppresses ROS levels and thereby blocks death (15), invoked the possibility that GO-203 induces death by a ROS-dependent mechanism. Indeed, as found previously with GO-201 (30, 31), treatment with GO-203 was associated with increases in ROS. By extension, the anti-oxidants NAC and Tiron attenuated GO-203-induced cell death, consistent with a ROS-mediated loss of survival. These findings would appear to support two effects of GO-203, one on PI3K signaling and the other on redox imbalance. Nonetheless, these results do not exclude the possibility that downregulation of the pro-survival PI3K->Akt pathway could contribute to increased sensitivity of these NSCLC cells to ROS-induced necrotic death. In this regard, Akt has been linked to the oxidative stress response and may exert its tumorigenic potential only after evading ROS-induced senescence (48, 49). Given these circumstances, the impact of GO-203 on NSCLC cell growth and survival in vitro provided the experimental basis for evaluating the anti-tumor activity of GO-203 against NSCLC xenografts growing in mice. Previous work has shown that murine lung carcinomas driven by a PI3K p110 mutant are highly sensitive to a dual PI3K-mTOR inhibitor (8). However, preclinical models suggest that PI3K or dual PI3K-mTOR inhibitors are likely to be less effective against lung cancers with EGFR mutations (4). In addition, mouse lung cancer driven by mutant K-Ras does not respond substantially to the dual PI3K-mTOR inhibitor (8). By contrast, our studies demonstrate that GO-203 is highly effective against H1975 cells with the EGFR(T790M) mutation, achieving complete responses that are maintained after completing 21 d of drug dosing. A549 K-Ras mutant tumors also responded to GO-203 with complete responses and lack of recurrence. These findings indicate that GO-203-induced inhibition of MUC1-C is effective against (i) NSCLC cells with wild-type EGFR and K-Ras in vitro, and (ii) NSCLC cells with mutant EGFR or K-Ras growing in vitro and in mouse models. Therefore, an agent, such as GO-203, that

NIH-PA Author Manuscript

NIH-PA Author Manuscript

NIH-PA Author Manuscript

targets MUC1-C and has entered Phase I clinical evaluation may be effective in the treatment of NSCLCs, including those with EGFR or K-Ras mutations.

Supplementary Material

Refer to Web version on PubMed Central for supplementary material.

Acknowledgments

Grant support: Lung Cancer Research Foundation and National Cancer Institute grants CA97098 and CA42802. The authors thank Dr. Pasi Janni for the H2228 cells.

References

1. Brognard J, Clark AS, Ni Y, Dennis PA. Akt/protein kinase beta is constitutively active in non-small cell lung cancer cells and promotes cellular survival and resistance to chemotherapy and radiation. Cancer Res. 2001; 61:3986–97. [PubMed: 11358816]
2. Lee HY, Oh SH, Suh YA, Baek JH, Papadimitrakopoulou V, Huang S, et al. Response of non-small cell lung cancer cells to the inhibitors of phosphatidylinositol 3-kinase/Akt- and MAPK kinase 4/c-Jun NH2-terminal kinase pathways: an effective therapeutic strategy for lung cancer. Clin Cancer Res. 2005; 11:6065–74. [PubMed: 16115952]
3. Kikuchi J, Kinoshita I, Shimizu Y, Oizumi S, Nishimura M, Birrer MJ, et al. Simultaneous blockade of AP-1 and phosphatidylinositol 3-kinase pathway in non-small cell lung cancer cells. Br J Cancer. 2008; 99:2013–9. [PubMed: 19018257]
4. Engelman JA. Targeting PI3K signalling in cancer: opportunities, challenges and limitations. Nat Rev Cancer. 2009; 9:550–62. [PubMed: 19629070]
5. Gupta S, Ramjaun AR, Haiko P, Wang Y, Warne PH, Nicke B, et al. Binding of ras to phosphoinositide 3-kinase p110alpha is required for ras-driven tumorigenesis in mice. Cell. 2007; 129:957–68. [PubMed: 17540175]
6. Guertin DA, Sabatini DM. Defining the role of mTOR in cancer. Cancer Cell. 2007; 12:9–22. [PubMed: 17613433]
7. Janne PA, Engelman JA, Johnson BE. Epidermal growth factor receptor mutations in non-small-cell lung cancer: implications for treatment and tumor biology. J Clin Oncol. 2005; 23:3227–34. [PubMed: 15886310]
8. Engelman JA, Janne PA. Mechanisms of acquired resistance to epidermal growth factor receptor tyrosine kinase inhibitors in non-small cell lung cancer. Clin Cancer Res. 2008; 14:2895–9. [PubMed: 18483355]
9. Kwak EL, Sordella R, Bell DW, Godin-Heymann N, Okimoto RA, Brannigan BW, et al. Irreversible inhibitors of the EGF receptor may circumvent acquired resistance to gefitinib. Proc Natl Acad Sci U S A. 2005; 102:7665–70. [PubMed: 15897464]
10. Riely GJ, Kris MG, Rosenbaum D, Marks J, Li A, Chitale DA, et al. Frequency and distinctive spectrum of KRAS mutations in never smokers with lung adenocarcinoma. Clin Cancer Res. 2008; 14:5731–4. [PubMed: 18794081]
11. Schiller JH, Adak S, Feins RH, Keller SM, Fry WA, Livingston RB, et al. Lack of prognostic significance of p53 and K-ras mutations in primary resected non-small-cell lung cancer on E4592: a Laboratory Ancillary Study on an Eastern Cooperative Oncology Group Prospective Randomized Trial of Postoperative Adjuvant Therapy. J Clin Oncol. 2001; 19:448–57. [PubMed: 11208838]
12. Pao W, Wang TY, Riely GJ, Miller VA, Pan Q, Ladanyi M, et al. KRAS mutations and primary resistance of lung adenocarcinomas to gefitinib or erlotinib. PLoS Med. 2005; 2:e17. [PubMed: 15696205]
13. Koivunen JP, Mermel C, Zejnullahu K, Murphy C, Lifshits E, Holmes AJ, et al. EML4-ALK fusion gene and efficacy of an ALK kinase inhibitor in lung cancer. Clin Cancer Res. 2008; 14:4275–83. [PubMed: 18594010]

NIH-PA Author Manuscript

NIH-PA Author Manuscript

NIH-PA Author Manuscript

14. Chen Z, Sasaki T, Tan X, Carretero J, Shimamura T, Li D, et al. Inhibition of ALK, PI3K/MEK, and HSP90 in murine lung adenocarcinoma induced by EML4-ALK fusion oncogene. Cancer Res. 2010; 70:9827–36. [PubMed: 20952506]
15. Kufe D. Mucins in cancer: function, prognosis and therapy. Nature Reviews Cancer. 2009; 9:874–85.
16. Ramasamy S, Duraisamy S, Barbashov S, Kawano T, Kharbanda S, Kufe D. The MUC1 and galectin-3 oncoproteins function in a microRNA-dependent regulatory loop. Mol Cell. 2007; 27:992–1004. [PubMed: 17889671]
17. Li Y, Ren J, Yu W, Li G, Kuwahara H, Yin L, et al. The EGF receptor regulates interaction of the human DF3/MUC1 carcinoma antigen with c-Src and β-catenin. J Biol Chem. 2001; 276:35239–42. [PubMed: 11483589]
18. Pochampalli MR, Bitler BG, Schroeder JA. Transforming growth factor {alpha} dependent cancer progression is modulated by MUC1. Cancer Res. 2007; 67:6591–8. [PubMed: 17638868]
19. Pochampalli MR, el Bejjani RM, Schroeder JA. MUC1 is a novel regulator of ErbB1 receptor trafficking. Oncogene. 2007; 26:1693–701. [PubMed: 16983337]
20. Li Y, Kuwahara H, Ren J, Wen G, Kufe D. The c-Src tyrosine kinase regulates signaling of the human DF3/MUC1 carcinoma-associated antigen with GSK3β and β-catenin. J Biol Chem. 2001; 276:6061–4. [PubMed: 11152665]
21. Pandey P, Kharbanda S, Kufe D. Association of the DF3/MUC1 breast cancer antigen with Grb2 and the Sos/Ras exchange protein. Cancer Res. 1995; 55:4000–3. [PubMed: 7664271]
22. Kinlough CL, Poland PA, Bruns JB, Harkleroad KL, Hughey RP. MUC1 membrane trafficking is modulated by multiple interactions. J Biol Chem. 2004; 279:53071–7. [PubMed: 15471854]
23. Raina D, Kharbanda S, Kufe D. The MUC1 oncoprotein activates the anti-apoptotic PI3K/Akt and Bcl-xL pathways in rat 3Y1 fibroblasts. J Biol Chem. 2004; 279:20607–12. [PubMed: 14999001]
24. Kato K, Lu W, Kai H, Kim KC. Phosphoinositide 3-kinase is activated by MUC1 but not responsible for MUC1-induced suppression of Toll-like receptor 5 signaling. Am J Physiol Lung Cell Mol Physiol. 2007; 293:L686–L92. [PubMed: 17586693]
25. Huang L, Chen D, Liu D, Yin L, Kharbanda S, Kufe D. MUC1 oncoprotein blocks GSK3beta-mediated phosphorylation and degradation of beta-catenin. Cancer Res. 2005; 65:10413–22. [PubMed: 16288032]
26. Ahmad R, Raina D, Trivedi V, Ren J, Rajabi H, Kharbanda S, et al. MUC1 oncoprotein activates the IκB kinase β complex and constitutive NF-κB signaling. Nat Cell Biol. 2007; 9:1419–27. [PubMed: 18037881]
27. Ahmad R, Raina D, Joshi MD, Kawano T, Kharbanda S, Kufe D. MUC1-C oncoprotein functions as a direct activator of the NF-kappaB p65 transcription factor. Cancer Res. 2009; 69:7013–21. [PubMed: 19706766]
28. Ahmad R, Rajabi H, Kosugi M, Joshi M, Alam M, Vasir B, et al. MUC1-C oncoprotein promotes STAT3 activation in an auto-inductive regulatory loop. Science Signaling. 2011; 4:ra9. [PubMed: 21325207]
29. Khodarev N, Ahmad R, Rajabi H, Pitroda S, Kufe T, McClary C, et al. Cooperativity of the MUC1 oncoprotein and STAT1 pathway in poor prognosis human breast cancer. Oncogene. 2010; 29:920–9. [PubMed: 19915608]
30. Raina D, Ahmad R, Joshi M, Yin L, Wu Z, Kawano T, et al. Direct targeting of the MUC1 oncoprotein blocks survival and tumorigenicity of human breast carcinoma cells. Cancer Res. 2009; 69:5133–41. [PubMed: 19491255]
31. Joshi MD, Ahmad R, Raina D, Rajabi H, Bubley G, Kharbanda S, et al. MUC1 oncoprotein is a druggable target in human prostate cancer cells. Mol Cancer Ther. 2009; 8:3056–65. [PubMed: 19887552]
32. Khodarev N, Pitroda S, Beckett M, MacDermed D, Huang L, Kufe D, et al. MUC1-induced transcriptional programs associated with tumorigenesis predict outcome in breast and lung cancer. Cancer Res. 2009; 69:2833–7. [PubMed: 19318547]
33. MacDermed DM, Khodarev NN, Pitroda SP, Edwards DC, Pelizzari CA, Huang L, et al. MUC1-associated proliferation signature predicts outcomes in lung adenocarcinoma patients. BMC Medical Genomics. 2010; 3:16. [PubMed: 20459602]

NIH-PA Author Manuscript

NIH-PA Author Manuscript

NIH-PA Author Manuscript

34. Gao J, McConnell MJ, Yu B, Li J, Balko JM, Black EP, et al. MUC1 is a downstream target of STAT3 and regulates lung cancer cell survival and invasion. Int J Oncol. 2009; 35:337–45. [PubMed: 19578748]
35. Shimamura T, Li D, Ji H, Haringsma HJ, Liniker E, Borgman CL, et al. Hsp90 inhibition suppresses mutant EGFR-T790M signaling and overcomes kinase inhibitor resistance. Cancer Res. 2008; 68:5827–38. [PubMed: 18632637]
36. Sordella R, Bell DW, Haber DA, Settleman J. Gefitinib-sensitizing EGFR mutations in lung cancer activate anti-apoptotic pathways. Science. 2004; 305:1163–7. [PubMed: 15284455]
37. Choi EJ, Ryu YK, Kim SY, Wu HG, Kim JS, Kim IH, et al. Targeting Epidermal Growth Factor Receptor–Associated Signaling Pathways in Non–Small Cell Lung Cancer Cells: Implication in Radiation Response. Mol Cancer Res. 2010; 8:1027–36. [PubMed: 20587532]
38. Sunaga N, Shames D, Girard L, Peyton M, Larsen J, Imai H, et al. Knockdown of oncogenic KRAS in non–small cell lung cancers suppresses tumor growth and sensitizes tumor cells to targeted therapy. Mol Cancer Ther. 2011; 10:336–46. [PubMed: 21306997]
39. Furugaki K, Iwai T, Shirane M, Kondoh K, Moriya Y, Mori K. Schedule-dependent antitumor activity of the combination with erlotinib and docetaxel in human non-small cell lung cancer cells with EGFR mutation, KRAS mutation or both wild-type EGFR and KRAS. Oncology Reports. 2010; 24:1141–6. [PubMed: 20878103]
40. Raina D, Ahmad R, Kumar S, Ren J, Yoshida K, Kharbanda S, et al. MUC1 oncoprotein blocks nuclear targeting of c-Abl in the apoptotic response to DNA damage. EMBO J. 2006; 25:3774–83. [PubMed: 16888623]
41. Guddo F, Giatromanolaki A, Koukourakis MI, Reina C, Vignola AM, Chlouverakis G, et al. MUC1 (episialin) expression in non-small cell lung cancer is independent of EGFR and c-erbB-2 expression and correlates with poor survival in node positive patients. J Clin Pathol. 1998; 51:667–71. [PubMed: 9930070]
42. Engelman JA, Chen L, Tan X, Crosby K, Guimaraes AR, Upadhyay R, et al. Effective use of PI3K and MEK inhibitors to treat mutant Kras G12D and PIK3CA H1047R murine lung cancers. Nat Med. 2008; 14:1351–6. [PubMed: 19029981]
43. Konstantinidou G, Bey EA, Rabellino A, Schuster K, Maira MS, Gazdar AF, et al. Dual phosphoinositide 3-kinase/mammalian target of rapamycin blockade is an effective radiosensitizing strategy for the treatment of non-small cell lung cancer harboring K-RAS mutations. Cancer Res. 2009; 69:7644–52. [PubMed: 19789349]
44. Faber AC, Li D, Song Y, Liang MC, Yeap BY, Bronson RT, et al. Differential induction of apoptosis in HER2 and EGFR addicted cancers following PI3K inhibition. Proc Natl Acad Sci U S A. 2009; 106:19503–8508. [PubMed: 19850869]
45. Songyang Z, Shoelson SE, Chaudhuri M, Gish G, Pawson T, Haser WG, et al. SH2 domains recognize specific phosphopeptide sequences. Cell. 1993; 72:767–78. [PubMed: 7680959]
46. Kufe D. Functional targeting of the MUC1 oncogene in human cancers. Cancer Biol Ther. 2009; 8:1201–7.
47. Shackelford DB, Shaw RJ. The LKB1-AMPK pathway: metabolism and growth control in tumour suppression. Nat Rev Cancer. 2009; 9:563–75. [PubMed: 19629071]
48. Chen Z, Trotman LC, Shaffer D, Lin HK, Dotan ZA, Niki M, et al. Crucial role of p53-dependent cellular senescence in suppression of Pten-deficient tumorigenesis. Nature. 2005; 436:725–30. [PubMed: 16079851]
49. Nogueira V, Park Y, Chen CC, Xu PZ, Chen ML, Tonic I, et al. Akt determines replicative senescence and oxidative or oncogenic premature senescence and sensitizes cells to oxidative apoptosis. Cancer Cell. 2008; 14:458–70. [PubMed: 19061837]

Abbreviations

NSCLC	non-small cell lung cancer
RTK	receptor tyrosine kinase

NIH-PA Author Manuscript

NIH-PA Author Manuscript

NIH-PA Author Manuscript

EGFR	epidermal growth factor receptor
PI3K	phosphoinositide 3-kinase
MUC1	mucin 1
MUC1-N	MUC1 N-terminal subunit
MUC1-C	MUC1 C-terminal subunit
MUC1-CD	MUC1-C cytoplasmic domain
ROS	reactive oxygen species

NIH-PA Author Manuscript

NIH-PA Author Manuscript

NIH-PA Author Manuscript

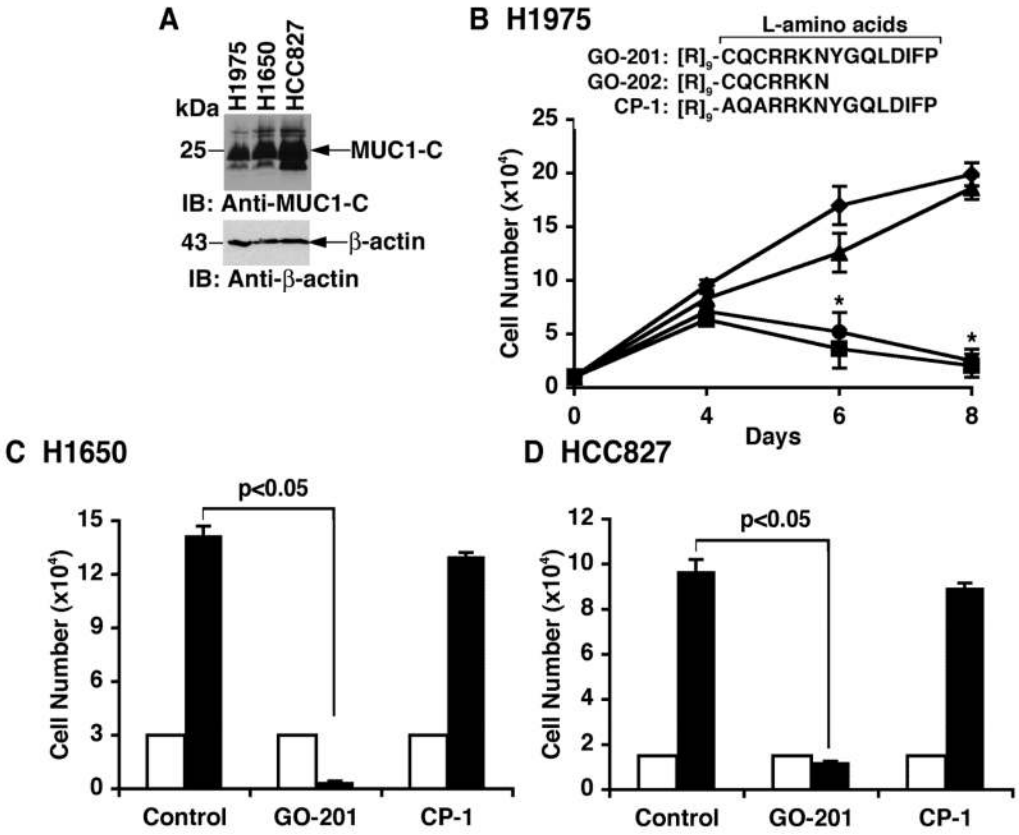

Figure 1. EGFR mutant NSCLC cells are sensitive to treatment with MUC1-C inhibitors

A. Lysates from the indicated NSCLC cells were immunoblotted with anti-MUC1-C and anti-β-actin. B. L-amino acid sequences of GO-201, GO-202 and CP-1. H1975 cells were left untreated (diamonds) and treated with 5 μM GO-201 (squares), GO-202 (circles) or CP-1 (triangles) each day for the indicated times. Viable cell number (mean±SE of three determinations) was determined by trypan blue exclusion. The asterisk (*) denotes a significant difference ($p<0.05$) from the untreated control. C and D. H1650 and HCC827 cells were left untreated (Control) and treated with 5 μM GO-201 or CP-1 each day for 6 days. Viable cell number (mean±SE of three determinations) on day 0 (open bars) and day 6 (solid bars) was determined by trypan blue exclusion.

NIH-PA Author Manuscript

NIH-PA Author Manuscript

NIH-PA Author Manuscript

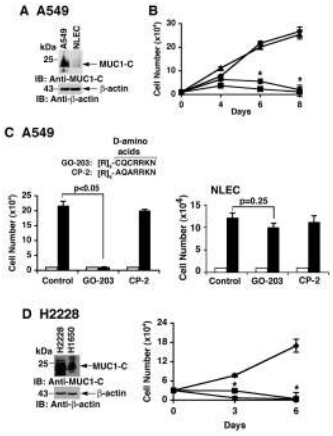

Figure 2. Growth of NSCLC cells with K-Ras and EML4-ALK mutations is inhibited by blocking MUC1-C function

A. Lysates from A549 (K-Ras G12S mutant) NSCLC cells and normal lung epithelial cells (NLEC) were immunoblotted with the indicated antibodies. B. A549 cells were left untreated (diamonds), and treated with 5 μM GO-201 (squares), GO-202 (circles) or CP-1 (triangles) each day for the indicated days (right). Viable cell number (mean±SE of three determinations) was determined by trypan blue exclusion. The asterisk (*) denotes a significant difference ($p<0.05$) from the untreated control. C. D-amino acid sequences of GO-203 and CP-2. A549 cells (left) and NLEC (right) were left untreated (Control) and treated with 5 μM GO-203 or CP-2 each day for 6 days. Viable cell number (mean±SE of three determinations) on day 0 (open bars) and day 6 (solid bars) was determined by trypan blue exclusion. GO-203 had no significant effect on NLEC growth as determined by the student's t-test ($p=0.25$). D. Lysates from H2228 (EML4-ALK mutant) and H1650 cells were immunoblotted with the indicated antibodies (left). H2228 cells were left untreated (diamonds), and treated with 5 μM GO-201 (squares) or GO-203 (triangles) each day for the indicated days (right). The asterisk (*) denotes a significant difference ($p<0.05$) from the untreated control.

NIH-PA Author Manuscript

NIH-PA Author Manuscript

NIH-PA Author Manuscript

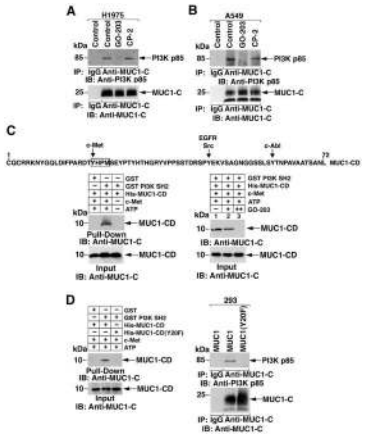

Figure 3. GO-203 blocks binding of the MUC1-C cytoplasmic domain to the PI3K p85 SH2 domain

A and B. H1975 (A) and A549 (B) cells were left untreated (Control), and treated with 5 μM GO-203 or CP-2 each day for 2 days. Lysates were precipitated with anti-MUC1-C or a control IgG. The precipitates were immunoblotted with anti-PI3K p85 and anti-MUC1-C. C. Amino acid sequence of the MUC1-C cytoplasmic domain (MUC1-CD). The indicated phosphorylation sites are highlighted and the YHPM is boxed. His-MUC1-CD was incubated with GST or GST-PI3K SH2 in the presence and absence of c-Met and ATP. GST or GST-PI3K p85 SH2 bound to glutathione beads was then added to the reaction products (left). c-Met-phosphorylated His-MUC1-CD was incubated with GST-PI3K SH2 in the absence and presence of increasing amounts of GO-203 (right). The adsorbates and inputs were immunoblotted with anti-MUC1-C. D. His-MUC1-CD and His-MUC1-CD(Y20F) were incubated with c-Met and ATP. GST or GST-PI3K p85 SH2 bound to glutathione beads was then added to the reaction products (left). The adsorbates and inputs were immunoblotted with anti-MUC1-C. 293 cells were transfected with vectors expressing MUC1 or MUC1(Y20F) for 48 h (right). Lysates were precipitated with a control IgG or anti-MUC1-C. The precipitates were immunoblotted with the indicated antibodies.

NIH-PA Author Manuscript

NIH-PA Author Manuscript

NIH-PA Author Manuscript

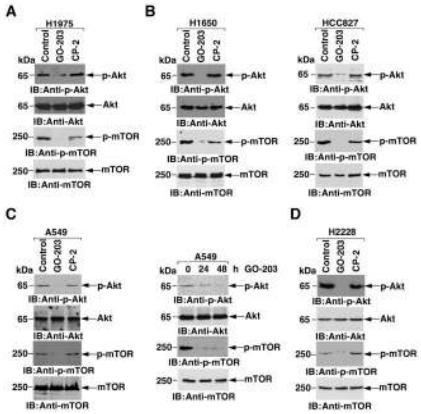

Figure 4. Inhibition of MUC1-C downregulates the PI3K->Akt->mTOR pathway

A. H1975 cells were left untreated (Control), and treated with 5 μM GO-203 or CP-2 each day for 2 days. Lysates were immunoblotted with the indicated antibodies. B. H1650 (left) and HCC827 (right) cells were left untreated, and treated with 5 μM GO-203 or CP-2 each day for 2 days. Lysates were immunoblotted with the indicated antibodies. C. A549 cells were left untreated, and treated with 5 μM GO-203 or CP-2 each day for 2 days. Lysates obtained at 48 h (left) and at both 24 and 48 h (right) were immunoblotted with the indicated antibodies. D. H2228 cells were left untreated, and treated with 5 μM GO-203 or CP-2 each day for 2 days. Lysates were immunoblotted with the indicated antibodies.

NIH-PA Author Manuscript

NIH-PA Author Manuscript

NIH-PA Author Manuscript

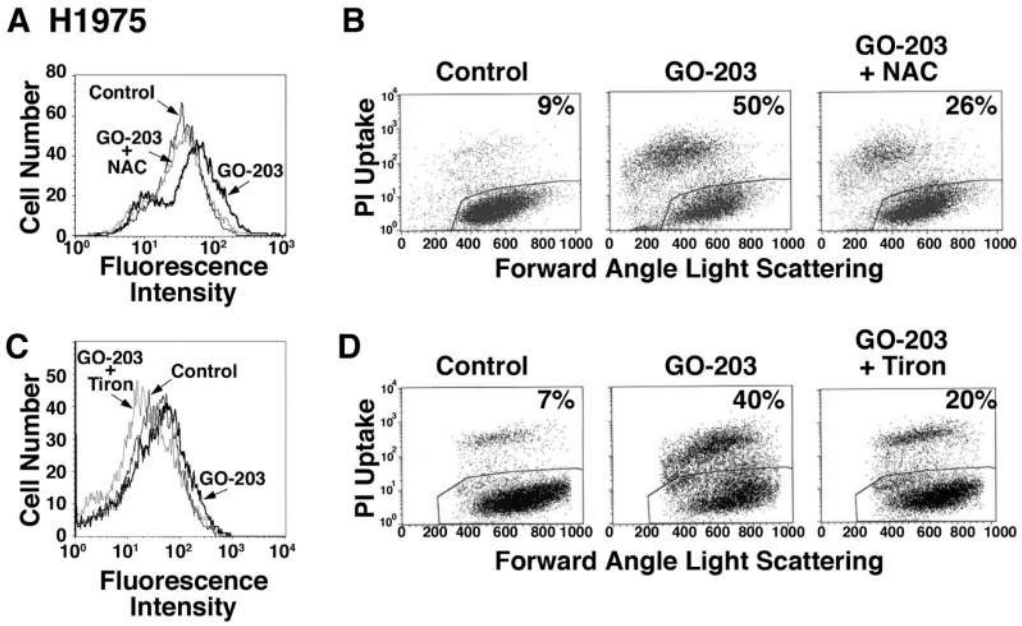

Figure 5. GO-203 induces death by a ROS-mediated mechanism

A. H1975 cells were left untreated (Control) and treated with 5 μM GO-203 in the absence or presence of 1 mM NAC for 3 d. The cells were then incubated with c-H_2DCFDA for 30 min, and fluorescence of oxidized c-H_2DCF was measured by flow cytometry. B. H1975 cells were left untreated (Control) and treated with 5 μM GO-203 in the absence or presence of 1 mM NAC for 5 d. Cells were stained with PI and analyzed by flow cytometry. The percentage of necrotic cells is included in the panels. C. H1975 cells were left untreated (Control) and treated with 5 μM GO-203 in the absence or presence of 5 mM Tiron for 3 d. The cells were then incubated with c-H_2DCFDA for 30 min, and fluorescence of oxidized c-H_2DCF was measured by flow cytometry. D. H1975 cells were left untreated (Control) and treated with 5 μM GO-203 in the absence or presence of 5 mM Tiron for 5 d. Cells were stained with PI and analyzed by flow cytometry. The percentage of necrotic cells is included in the panels.

NIH-PA Author Manuscript

NIH-PA Author Manuscript

NIH-PA Author Manuscript

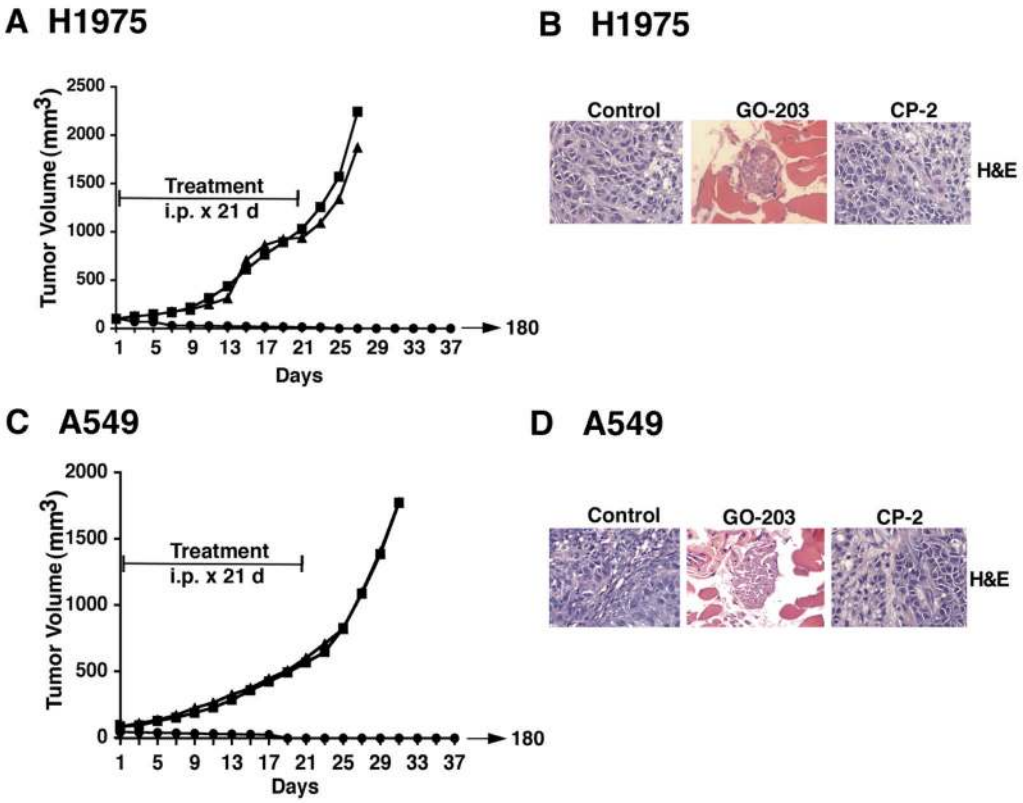

Figure 6. GO-203 is effective in the treatment of H1975 and A549 tumors

A-D. BALB/c nu/nu mice were injected subcutaneously in the flank with 1×10^7 H1975 or A549 cells. The mice were pair matched when the H1975 and A549 tumors were 100-125 and 60-75 mm^3, respectively. Treatment groups consisted of 10 mice injected intraperitoneally with PBS (vehicle control; closed squares), 30 mg/kg GO-203 (closed circles) or 30 mg/kg CP-2 (closed triangles) each day for 21 d. Mice were weighed twice weekly and tumor measurements were performed every 2 d. There was no weight loss in any of the groups. The results are expressed as the mean tumor volume with a SE of <20% (A, C). H1975 and A549 tumors were harvested from the control and CP-2-treated mice at the time of sacrifice. H1975 and A549 tumor implantation sites from the GO-203-treated mice were harvested on day 32 and 36, respectively. Tissues were stained with H&E (B, D).